Assessing the removal mechanisms of engineered nanoparticles in aerobic granular sludge systems

Pedro Miguel Teixeira da Silva
pedromtsilva@tecnico.ulisboa.pt

Abstract

The textile industry stands as one of the most polluting industrial sectors, being one of the main causes of water pollution, especially in underdeveloped countries. Due to their antimicrobial properties, the application of silver nanoparticles (AgNPs) in this industry has been increasing and their occurrence in wastewater is expected to rise accordingly. Wastewater treatment plants can act as important barriers to prevent nanoparticles from reaching the environment. In this study, two sequencing batch reactors (SBRs; one AgNP-fed and one AgNP-free control) operating with aerobic granular sludge (AGS) were monitored during a 16-week period with the main purpose of assessing the impact of AgNPs on the performance of the AGS SBR system and their possible removal mechanisms. Due to the important role of extracellular polymeric substances (EPS) in the AGS stability, the polysaccharide and protein contents of EPS were characterized. Polysaccharides were the EPS major component. The presence of AgNPs did not significantly influence the EPS protein content, but polysaccharide content consistently decreased by report to control SBR. Nonetheless, AgNPs appeared to have no toxic effect on AGS as the Ag-fed SBR consistently presented a higher proportion of granular biomass and a better overall performance. AgNPs proved to be substantially retained in AGS. Imaging the elemental distributions across granule sections revealed a preferential deposition of Ag at the periphery of the granule and a sharp decrease towards inner regions. It was also demonstrated that granules exposed to AgNPs exhibited significant differences in the distribution profile of essential and trace elements.

Keywords: Textile wastewater; Aerobic granular sludge; Sequencing batch reactor; Silver nanoparticles; Extracellular polymeric substances; Elemental mapping.

Introduction

Currently, the textile industry moves billions of dollars worldwide and assumes an important position in the world economy, playing a critical role in the industrial development of some countries such as China, India, Pakistan, Bangladesh and Malaysia [1]. As of 2015, China, the European Union and India were the top three textile exporters, representing 66.4% of total textile exports around the globe [2]. The utilization of nanoparticles, namely AgNPs, to confer antimicrobial activity in different textile materials is currently fairly common. This silver-based compounds are among the main antimicrobials used in textiles[3]. Due to the good antimicrobial properties of AgNPS, their use in the textile industry rapidly increased and their significant occurrence in wastewater is now a worrying issue [3–5].Not much is known about the fate of AgNPs during exploitation and maintenance of textile goods. Thus, information on the amount and form of AgNPs released into wastewater still needs to be unveiled, and gathered knowledge would be critical to assess the potential environmental risks [6].

Sequencing batch reactor (SBR) systems have been regarded as attractive for industrial wastewater treatment applications[7]. Offering a compact layout, operational flexibility and simplicity [8], SBR systems can be operated with aerobic granular sludge (AGS). The biomass granules in AGS are densely packed microbial aggregates, mainly composed of bacteria, and extracellular polymeric substances (EPS). These structures can be described as spherical biofilms in suspension and their densities are much higher than the ones of conventional activated sludge [9].

Being one of the main components of AGS [9], EPS not only plays a key role in the formation of a gel-like network that keeps bacteria together in biofilms, but also protects bacteria against noxious environmental conditions and can even serve as carbon or energy sources in nutrient limitation conditions [10–12]. EPS acts as a permeability barrier having a protective effect relative to heavy metal exposure by blocking their direct interaction with cells and eventual intracellular penetration. It was recently demonstrated that EPS can biosorb both Ag+ and AgNPs, mitigating the well documented antibacterial activity of Ag+ [12,13].

Due to the small size of nanoparticles, their localization and quantification in biological media and within cells are extremely challenging issues. Therefore, various cutting-edge techniques are required to detect and to quantify the metal content in biological materials, which comprise the nanoparticle fraction, such as AgNPs. Nuclear microscopy, combines several ion beam analytical techniques in order to obtain nano-micro-sized 2 dimensional (2D) images of the sample morphology and elemental distribution with depth information extracted from the calculated beam energy loss [14–17]. By simultaneously using techniques such as: STIM (scanning transmission ion microscopy), PIXE (proton induced X-ray emission) and RBS (Rutherford backscattering spectrometry) it is possible to extract spectral information to produce images of sample features and quantify elemental contents in the sample. Therefore, these techniques can provide unique information concerning nanoparticles distribution in biological media.

The major aim of this study was to characterize the interaction of AgNPs with a AGS system. One of the focal points was the assessment of the AgNPs long-term exposure effects and spatial distribution within a AGS system. Two SBRs were set up in the same operational conditions, one supplemented with AgNPs and the other used as AgNP-free control, and their performance was consistently evaluated. Efforts were made to determine the concentration of AgNPs in granular sludge structures, in the monitored SBR systems. The effects of the exposure to AgNPs on the total EPS content of the biomass were also subject of investigation.

Methods

Experimental layout and SBR cycle operation

The experimental system included two bubble-column SBRs, SBR1 and SBR2. Both reactors had a working volume of 1.5 L (height/diameter ratio of 2.5) and were set-up in identical conditions, except that at the end of each fill phase, SBR1 was supplied with AgNPs (<100 nm) whereas SBR2 was used as AgNPs-free control. The following operational parameters were adopted: 6-h cycles (12-h HRT) with 5 sequential phases, namely, fill (30 min), react (anaerobic and aerobic, 1.5h and 3.5h respectively), settle (5 min), drain (1 min) and idle (30 min).

The SBRs were inoculated with the same biomass composed by activated sludge flocs (1.4 g TSS/L) harvested from a full scale, conventional municipal wastewater treatment plant (Chelas, Lisboa, Portugal). The SBRs were fed with a synthetic textile wastewater provided separately as carbon feed solution (Feed-C) and nitrogen dye-containing feed solution (Feed-N) to minimize the risk of contamination, with an exchange ratio of 50% and a volumetric organic loading rate (OLR) of 2.0 kg COD / (m^3.d).

Peristaltic pumps (Mini-S 660, Ismatec, Switzerland) were used to feed the synthetic wastewater to the reactors, and after AGS settling, the drain of the supernatant was achieved using gear pumps (Reglo-Z, Ismatec, Switzerland). Mechanical mixing during the non-aerated reaction was provided by magnetic stirring using an anchor-like impeller at 70 rpm. During the aerobic reaction, aeration (2 v.v.m) was supplied through air compressors (SPP-20 GJ-L, Hiblow, Japan) via a porous membrane diffuser at the bottom of each bioreactor. The pumping, aeration and agitation functions were automatically controlled, via an interface, by a dedicated software.

Simulated textile wastewater

The Feed-C solution was prepared by diluting the carbon source stock solution (100 g/L) in distilled water to a COD content of 1000 mgO_2/L (1.15 g/L Emsize E1) and supplemented with the following nutrients: $CaCl_2$ (27.5 mg/L); $MgSO_4$•$7H_2O$ (22.5 mg/L); $FeCl_3$•$6H_2O$ (250 µg/L). Emsize E1 (Emsland-Starke GmbH, Germany) is a potato-starch-based sizing agent used in the textile industry. One litre of stock solution is obtained by dissolving 100 g of Emsize E1 and 40 g of sodium hydroxide in 500mL distilled water and stirring for 15 hours at room temperature. At that point the hydrolysed solution is neutralized to pH 7 with 80 mL HCl (37%) and diluted with distilled water to make up a final volume of 1L.

The Feed-N solution was prepared by diluting in distilled water phosphorus and nitrogen salts, an azo dye (AR14, Chromotrope FB, Sigma Aldrich, 50% dye content) and other micro-nutrients. The dissolved components were: Na_2HPO_4•$12H_2O$ (2.31 g/L); KH_2PO_4 (762 mg/L); NH_4Cl (143 mg/L); AR14 Chromotrope FB, Sigma Aldrich, 50% dye content (40 mg/L); $MnSO_4$•$4H_2O$ (40 µg/L H_3BO_3 (57 µg/L); $ZnSO_4$•$7H_2O$ (43 µg/L) and $(NH_4)_6Mo_7O_{24}$•$4H_2O$ (35 µg/L). The dye stock solution was prepared by dissolving AR14 in distilled water to a final concentration of 5.0 g/L. The AR14 concentration at the onset of the reaction phase (after the fill phase) was 20 mg/L.

The AgNPs suspension was prepared by diffusing 100mg AgNP nanopowder (<100 nm particle size, Sigma Aldrich) in 1L milli-Q water using sonication (60 minutes at 80W) to promote nanoparticle dispersion. After sonication, this suspension was diluted with 1L milli-Q water to a final concentration of 50 mg/L. The concentration of AgNPs in SBR1 at the onset of the reaction phase (after the fill phase) was 10 mg/L.

Extracellular polymeric substances (EPS) analysis

For both protein (PN) and polysaccharide (PS) fractions in EPS, the sampling was performed by weekly retrieving 5 mL sample duplicates along the reaction phase of one treatment cycle. These samples were dewatered by centrifugation at 4000 rpm for 10 min (discarding the soluble EPS fraction). The obtained pellets were immediately covered in EPS extraction buffer solution (2 mM $Na_3PO_4 \cdot H_2O$, 4 mM $NaH_2PO_4 \cdot 12H_2O$, 9 mM NaCl, 1 mM KCl, pH 7) to the original volume. The samples were kept at 4ºC until further analysis. The pellet resuspension was performed by mixing vigorously with a pipette until a homogeneous sludge suspension was obtained immediately before the extraction procedure.

The extraction of the bound EPS from sludge samples was carried out by heating the mixture suspensions to 80°C for 30 min in a water bath. Then, the suspensions were cooled down to room temperature and centrifuged at 4000 rpm for 20 min. Prior to EPS component analysis, the supernatant was further filtered through glass microfiber filter discs (Whatman, GF/C, ø 25 mm).

The PN content was determined with Pierce® BCA protein assay kit (Thermo Scientific, USA) using bovine serum albumin (BSA) as standard after a purification step by precipitation. For protein precipitation a modified method of trichloroacetic acid (TCA) was applied [18]. The PS content was analysed in accordance to the method described in Dubois, Gilles, Hamilton, Rebers, & Smith (1956) with some minor modifications.

Elemental distribution and quantification

Sample preparation for nuclear microscopy

In order to access the AgNPs distribution across the granule, samples of mixed liquor (2 mL) were collected from SBR1 and SBR2 during the anaerobic phase of the reaction step along different days in the same operational period. With the help of a magnifier glass granules were manually isolated and enclosed in a resin-like material (OCT™ compound). At this point the enclosed granules were quench-frozen in liquid nitrogen and sectioned in a cryotome (-22ºC working temperature) (Cryotome 620E, Termo Shandon, Cheshire, UK). The attained granule-containing sections with 20 µm thickness were allowed to dry overnight in the cryostat. The obtained sections were kept in petrislides™ and stored at -80ºC until analysis. For nuclear microscopy analysis, the preserved sections were mounted in appropriate frames in a self-supporting mode hold by the edges in carbon conductive adhesive tape (Agar Scientific, UK).

Sample preparation (for PIXE and ICP-MS)

To quantify Ag in reactor mixed liquor and effluent fractions, duplicate 5mL samples were retrieved from SBR1 and SBR2, as well as from the respective effluents and AgNPs feed solution. Total AGS samples, biomass and supernatant fractions and effluent were analysed using two techniques according to sample characteristics. Solid fractions or residues obtained by lyophilization, filtration, or centrifugation were analysed by PIXE, whereas liquid fractions (supernatants and filtrates) were analysed by ICP-MS.

To obtain biomass and effluent fractions, samples collected from the reactor and samples of the effluent, except the AgNPs feed, were filtered using polycarbonate filters of 0.2 µm pore (Whatman® Nuclepore™ Track-Etched Membranes) in order to separate the solid and liquid fraction. Biomass fraction was retained in the filters, which were stored in Petri slides dried in a freeze dryer (Edwards, USA) and stored at -80ºC until further study. Depending on the amount of biomass fractions

retained in the filters sample preparation for Ag concentration determination by PIXE may differ. If the biomass amount was large and it detaches from the filter, it has to be homogenized by shaking vigorously the material. The homogenized sample is then pelletized using 10 Ton pressure. If the biomass amount was adherent to the filter it can be analysed directly. Filters were weighed before use and after filtration to obtain the mass filtered (wet and dry mass). Volume filtered was also controlled therefore Ag concentrations can be expressed in both dry mass and volume fractions.

The liquid fractions of the filtered samples (from the reactor and effluent) were acidified with 10% v/v HNO_3 (suprapure) and homogenized in ultrasound bath at 40ºC for 3 cycles of 1h each. Samples were stored at -80ºC until further analysis. The sample preparation for Ag determination by ICP-MS required filtration before analysis (Whatman Swinnex filter of 0.2 µm pore), dilution and addition of an internal standard. For ICP-MS analysis, the filtered samples were diluted at least 2-fold with ultrapure water to obtain solutions of 5% HNO_3 (v/v) which were adequate for analysis. Subsequent dilutions whenever needed were done using acidified 5% (v/v) HNO_3 ultrapure water. Samples were doped with Y (Yttrium) as an internal standard at a concentration of 10µg/L.

Total AGS aliquots and AGS pellets obtained by centrifugation (4000 rpm, 10 min) were also analysed by PIXE. These samples were first freeze-dried and subjected to acid digestion with a mixture of H_2O_2 and HNO_3 (Merck suprapure reagents) in a proportion of 100 mg of sample to 200 µL of H_2O_2 and 2400 µL of HNO_3. The digestion was carried out in Teflon Bombs (Parr, Inc, USA) using a commercial microwave (Miele^{TM}) at 300 W during 4 min. From the resulting solution 10 µL were deposited onto a polycarbonate film and analysed, as described elsewhere [20,21].

Stock solution of 1000 ± 10 µg/L of Y (AAS Specpure Y solution; Alpha Aesar,Ward Hill, MA,USA) was used for internal standardization and preparation of spiked samples. Ultrapure water of 18 MΩ·cm (Milli-Q Element; Millipore, Billerica, MA, USA) was used for dilution of samples, stock solutions and to prepare blank solutions. Concentrated suprapur nitric acid (HNO_3) high-purity grade was obtained from Merck (Darmstadt, Germany).

Data acquisition

The Nuclear microscopy and PIXE technique are implemented at the Van de Graff accelerator of the CTN/IST. A proton beam of 2.0 MeV was used and the analyses were all performed in vacuum. In the nuclear microscopy set-up the data acquisition and map construction is carried out with OMDAQ whereas spectra analysis and quantitative determination of elemental contents[22] was performed with DAN32 computer code. PIXE spectra were analysed with AXIL program[23], and the concentration calculations performed with the computer code DATTPIXE as described elsewhere [24].

The ICP-MS equipment, ELAN DRCe (PerkinElmer, SCIEX, Waltham, MA, USA) available at CTN/IST was operated at 1100 W, with argon gas flow of 15 L/min and 0.85 aerosol L/min gas carrier using a Peltier-cooled cyclonic spray chamber. Data acquisition was done at peak-hopping mode with 50 ms dwell time, 20 sweeps/reading, 1 reading/replicate, and 3 replicates. Quantitative analysis was carried out based on an external calibration using Y as an internal standard. Data were collected, processed, and analysed with ELAN 3.4 software.

Results and Discussion

SBR cycle monitoring

The SBRs were monitored once a week with parameters such as TSS, VSS SVI, COD removal, colour removal and, pH being studied. The quantification of mass fractions was also performed. SBR1 consistently presented higher TSS and VSS values, and higher granular biomass content, resulting in better settling (results not shown). SBR1 also presented higher COD removal (Figure 1)

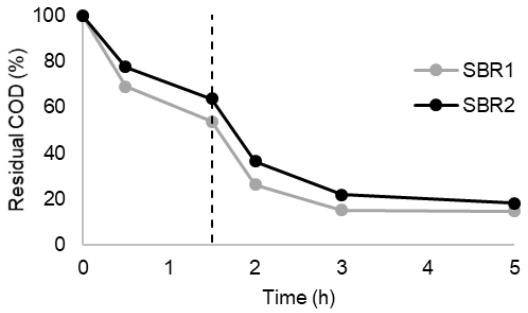

Figure 1 COD removal profile across a representative SBR cycle (data relative to operational day 240). The vertical line indicates the onset of aeration.

Extracellular polymeric substances analysis

Seven cycles of each SBR were monitored with the AGS being analysed for PN and PS total content (per unit of biomass) in extracted EPS, from now on referred only as PN and PS content, respectively. The first monitored cycle (operational day 191) was before an 18-day interruption, where the biomass was stored at 4ºC in closed glass containers, with all typical procedures involving the regular bioreactor functioning being interrupted during this period. The remaining cycles occurred after the mentioned interruption.

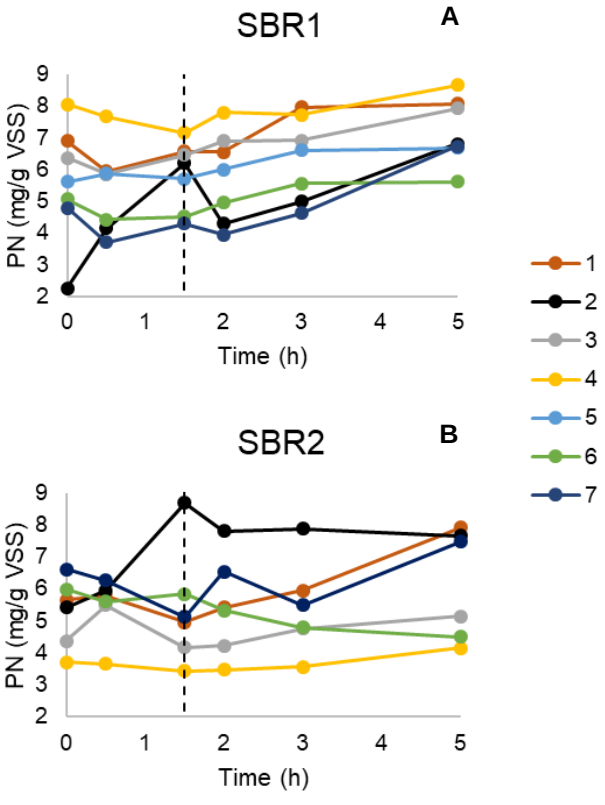

Figure 1 Evolution of the protein content in SBR1 (A) and SBR2 (B) across the reaction period of different cycles (1-7, monitored chronologically). The vertical line indicates the onset of aeration.

The SBRs presented a PN content somewhat errant (Figure 2), values ranging from 2.3 to 8.7 (mg/g VSS) for SBR1 and from 3.4 to 8.7 (mg/g VSS) for SBR2. The first cycle after reactivation (cycle 2) was the one with the most variable profile in both SBRs, increasing significantly during the cycle anaerobic phase, then decreasing on the onset of aeration and resuming the increasing tendency in the remaining period of the aerobic reaction phase. However, contrarily to SBR1, where cycle 2 presented values in accordance to the ones measured in the remaining cycles, in SBR2 the homologue cycle had significantly higher PN content than the remaining ones, across most of the cycle duration. This might be justified by the fact that the initial PN content in SBR1 cycle 2 was very low after the storage period, while the cycle 2 in SBR2 had a starting point value similar to the presented in the remaining monitored cycles. One can assume that although both reactors presented a PN content recovery along cycle 2, more PN was consumed by the biomass of SBR1 during the storage period, as the starting point of this latter one was in line with the values measured in the remaining cycles.

The increase of PN content verified immediately after storage might be related to the higher COD removal in the same period. Some patterns of aerobic granules-associated EPS during an SBR cycle have already been described and were credited to the applied feed regime. The existence of a short substrate feast phase and a relatively long famine phase would greatly influence both the PN and PS [25–27]. The EPS content would increase in the periods where COD removal was more significant. This way, an increase of PN and PS content was expected right after de fill phase, in the anaerobic portion of the reaction phase where most COD was removed. The use of EPS as a source of carbon and energy by some microorganisms during the famine phase was also reported [28–30]. Thus, the reduction of EPS content was expected in the aerobic phase.

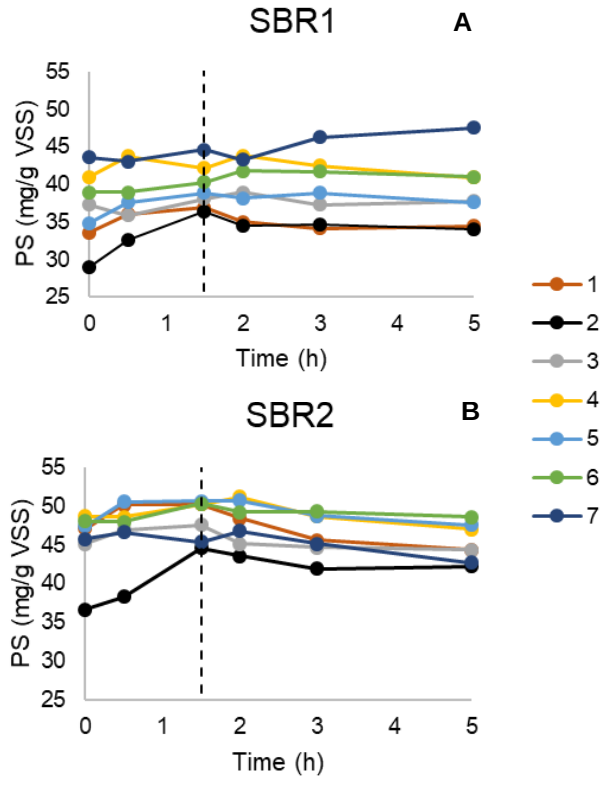

Figure 2 Evolution of the polysaccharide content in SBR1 (A) and SBR2 (B) across the reaction period of different cycles (1-7, monitored chronologically). The vertical line indicates the onset of aeration.

Overall, the results for PS content (Figure 3) appear to be less variable that the ones for PN. The obtained values ranged from 29.1 to 47.5 and 36.6 to 51.2 (mg/g VSS) for SBR1 and SBR2 respectively. Overall, SBR2 presented a slight higher PS content than SBR1. It is possible to perceive that the evolution of the PS content in the majority of the monitored cycles, unlike what was verified in the PN quantification, appeared to present a stable pattern. The PS content increased slightly in the anaerobic phase and slightly decreased with aeration. Once again, this is in agreement with previously reported results [25–27] that showed an EPS increase in the periods where COD removal was more significative, in our case during the anaerobic portion of the reaction phase (Figure 1). The subsequent consumption of EPS was also described, as these substances were used as carbon and energy source by some microorganisms during the famine phase[28–30]. Thus, a reduction in the EPS content was expected during the aerobic phase. This behaviour was observed regarding the PS content but not the PN content. The PS content production and consumption processes across the SBR cycle appear to be closely related to the external substrate availability.

In order to evaluate the evolution of PN and PS content across a larger time frame, and since a cycle was monitored per week, the average values were calculated for each monitored cycle. Figure 4 presents the average PN and PS content for each week-representing cycle.

It is possible to see that SBR1 has a significantly different profile from SBR2 (Figure 4). SBR1 appeared to have consumed PN during the storage period and recovered in the following weeks. SBR2 presented the exact opposite profile.

Despite the different relative biomass size fractions of the mixed liquor in the two SBR, the results regarding the average PN content (mg/g VSS) in each SBR cycle were in the same range (varying from 4.7 to 7.8 and 4.7 to 7.2 for SBR1 and SBR2 respectively). Neither the AgNPs presence nor the different percentages in biomass size fractions, namely flocculent and granular, appeared to have contributed to a difference in the quantification of PN. Both SBR1 and SBR2 presented the highest values in different periods of the monitored operation (Figure 4), leading to the idea that the displayed variations were caused by the specific reactor dynamic, rather than a particular tendency caused by an external factor (AgNPs).

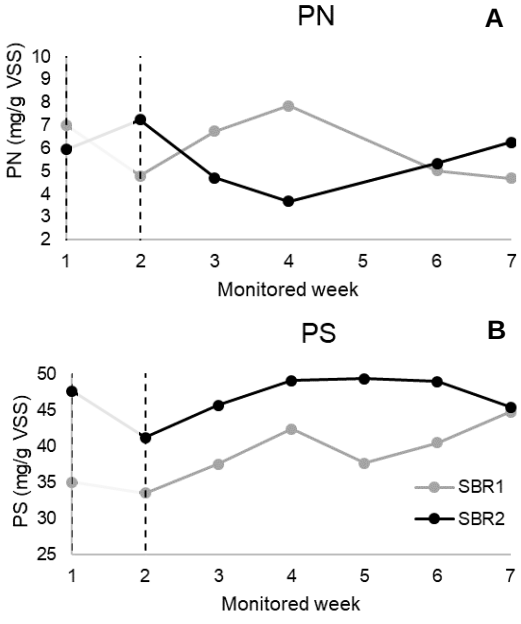

Figure 3 Average PN (A) and PS (B) content for each week-representing cycle. Note that between monitored week 1 and monitored week 2 lays the 18-day storage period, graphically delimit by the vertical lines.

Considering Figure 4B, the two SBRs studied showed, at some degree, depletion in PS content from the first to the second cycle and then, although with differing patterns, they both increased, clearly indicating a recuperation period after which the initial values were attained or passed. According to these average cycle values, PS appeared to be consumed during the storage period (between monitored week 1 and 2), thus corroborating the published studies [28,30].

Given that the results are normalized to mixed liquor VSS content, one can hypothesize that the numerical differences between the calculated PS content are most likely caused by the different morphological states of the biomass in the mixed liquor. The results already contemplate the difference in the amount of biomass present in the reactors, however, different granulation stages can cause alteration in the results. The PS content (mg/g VSS) in the totality of monitored cycles varied from 33.5 to 44.7 and 41.2 to 49.3 for SBR1 and SBR2, respectively, averaging 38.8 and 46.7 mg/g VSS, corroborating previously reported results where flocculent biomass presented a higher relative PS content [31]. (Figure 4B). It could be expected that the biomass from the Ag-fed SBR1 presented higher EPS content in order to capture AgNPs, but it did not occur. The PS content appeared to vary more significantly due to the granulation fraction in the biomass present in each bioreactor.

The combined analysis of the EPS components content showed PN/PS ratios around 0.15 and 0.12 for SBR1 and SBR2, respectively. According to these values, the content of PN was much higher than that of PS and the presence of AgNPs seemed to have no evident effect. For a variety of biofilm types and EPS extraction methods, in the majority of the published studies, proteins have been reported as more abundant than polysaccharides in EPS [11,32–34]. There is, nonetheless, contradictive bibliography where the PS content appeared dominant over the PN content [35], raising the hypothesis that PS contributed more to granule structure and stability than the PN. Thus, there are no typical values for granular biomass PN/PS ratio, but overall, bibliography indicates that PN is the most abundant EPS component in granular biomass.

Given these considerations, the herein obtained results regarding PN/PS ratios are very low. The small percentage of actual granular biomass present in the bioreactors definitely contributes to low PN/PS values, as these have been associated with non-granular biomass. The data concerning the mass fractioning indicated maximum values of only 25% and 4% of granular biomass in SBR1 and SBR2, respectively. Additionally, the low results obtained could also mean that the independent quantification of the EPS components was consistently miscalculated, most likely due to a low and selective extraction efficiency. This way, the underestimation of protein content is also a real possibility. Despite the efforts to optimize the extraction and quantification of EPS components, further studies are needed to attain more reliable procedures, especially concerning PN content.

Elemental spatial distribution using nuclear microscopy

Ag spatial distribution

This assay provided a sectional view of the AGS morphology. The sections of AGS derived granules were analysed under nuclear microscopy. The preferential peripheral distribution of Ag in AGS granules is evident. Other elements were also detected in considerable quantities such as P, S, K, Ca, Mn and Fe, which distributed non-uniformly. The deposition of AgNPs appears to occur in agglomerates, which can be easily visualised in the granule peripheral region. The fact that Ag is not evenly distributed throughout the granule goes in accordance with the reported affinity of EPS for metals[12,30,36,37]. Although presenting a clear peripheral distribution, Ag was also sporadically found in inner regions of the sectioned granule. The distribution of the structural element P (Figure 5D) emphasise a porous-like organization and the scarcer Ag detection in inner regions of the granules seem to be in their vicinity (Figure 5C)

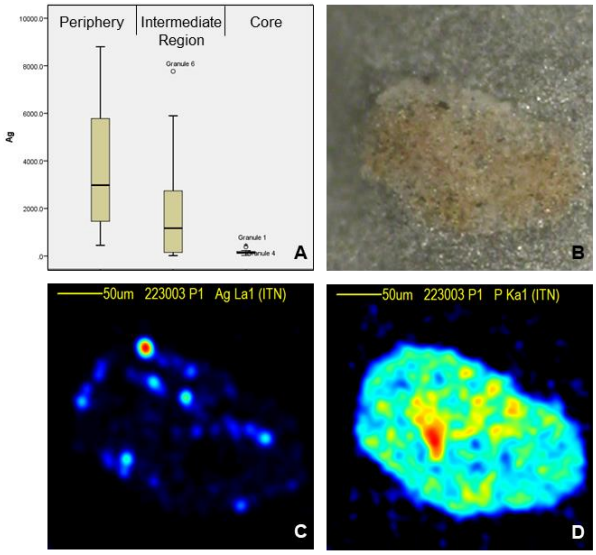

Figure 5 Box plot of Ag concentration in the three defined AGS regions (pheriphery, intermediate region and core) (A). Optical microscopy image of a AGS section (B) and corresponding Ag and P maps (C-D): The content gradient is represented by a dynamic colour scale: low–blue to high–red. In (A) the box represents the 25% and 75% interquartiles (IQ) and the dividing horizontal line indicates the median; whiskers indicate the maximum and minimum value.

Overall elemental composition

A wide-ranging dataset comprising the estimated elemental composition of each point of interest in all analysed granules of each reactor was created. Several sections of both Ag-fed (SBR1) and Ag-free (SBR2) granules were inspected, being the median concentration values of the studied elements examined according to three regions of the granules, i.e., periphery, intermediate region and core. The elemental concentration differences, between the control SBR2 and the AgNPs-fed SBR1 were then studied and their significance calculated, using Mann-Whitney non-parametric test (Table 1).

Overall micro-PIXE analysis showed that absolute concentration values for structural elements were higher in SBR1, and that micronutrients concentrations were higher in the granules retrieved from the control bioreactor, especially at the periphery. Analysing the concentration variations (%) of the AgNPs-feed SBR1 relative to the control SBR2, the P, K and Ca elemental concentrations significantly increased ($p<0.05$) in the intermediate and core regions. Opposite, the concentrations of the micronutrients Mn, Fe and Zn showed a significant decrease ($p<0.05$) in the periphery region of AgNPs-feed SBR.

Table 1. Absolute median concentration values (mg/kg dry mass) of the studied elements in the three regions of the granule. The significant concentration variations of SBR1 relative to SBR2 (%) are also indicated.

		Elemental concentration							
		Structural elements				Micro nutrients			Ag
		P	S	K	Ca	Mn	Fe	Zn	
AgNPs (SBR1)	Periphery	14202	6546	3207	2444	18	124	58	2978
	Intermediate	16664	9748	5136	3073	21	138	82	1168
	Core	17793	10943	5428	3736	22	130	87	141
CTR (SBR2)	Periphery	12217	6820	2176	3189	28	265	162	-
	Intermediate	7232	4953	1622	1829	12	141	110	-
	Core	6147	8732	2066	2178	16	170	150	-
Variation (%)*	Periphery	-	-	-	-	-36%	-53%	-64%	-
	Intermediate	+130%	-	+217%	+68%	-	-	-	-
	Core	+189%	-	+163%	-	-	-	-	-

*Only significant values are presented ($p<0.05$)

The Ag distribution in granules of SBR1 showed a massive deposition at the periphery with a sharp decrease to intermediate regions of the granule. The core of the granules was practically void of Ag. It is possible that the AgNPs preferentially accumulated in the peripheral region, possibly leading to the concentration reduction of other elements in this area, namely micronutrients. The chelating properties of EPS are well described [38], being these substances essential for biomass to capture free nutrients in the surrounding media. Perhaps the high load of AgNPs that the tested biomass underwent may have hampered the association of EPS with other nutrients existing in a much smaller quantity. The disparity in the proportion of AgNPs and other metals in the media may have caused some sort of competition between the AgNPs and free micronutrients, such as Mn, Fe and Zn.

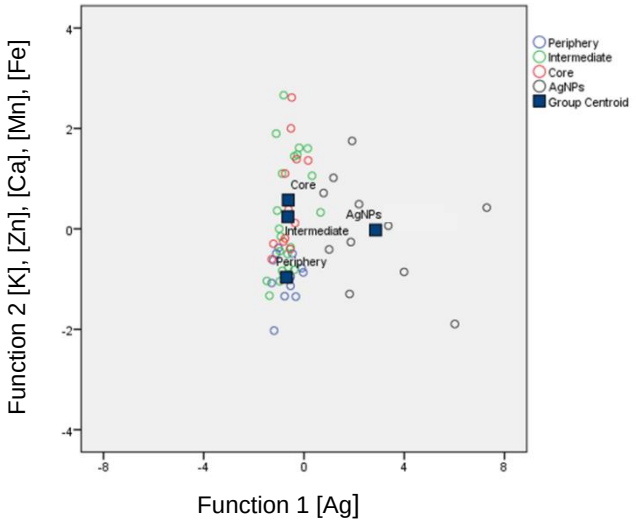

Figure 6 Canonical discriminant function, illustrating the elemental similarity degree between the three studied regions i.e., periphery, intermediate and core. An extra group (AgNPs) is also presented comprising large agglomerates of Ag. The first function expresses mostly the variance associated with Ag while the second function express the variance of K, Zn, Ca, Mn, Fe.

The AgNPs-feed granules showed higher contents of structural elements, such as, P, K and Ca, in the inner regions than the control. The presence of these elements in biological systems is strongly linked to an active metabolic activity. In some way the granular communities may be trying to compensate the micronutrient depletion in the more peripheral areas of the AGS, by producing more biomass that would ultimately produce more EPS maximizing the capture abilities. Moreover, this hypothesis explains the not so clear fact that the AgNPs exposed granules present higher development stage and biomass content.

A discriminant analysis was performed and the studied data revealed that the peripheral region could be clearly distinguished from the remaining intermediate and core regions that sit close together, indicating a large degree of similarity. (Figure 6). These results corroborate the findings described above, especially that the periphery region has distinct characteristics from inner regions, independently of the presence of Ag. Structural elements and micronutrients, such as K, Ca, Mn, Fe and Zn, enabled discriminating the outer layers of the granule from inner regions.

Quantification of Ag in reactor (bulk) mixed liquor and effluent fractions

Whilst the previous chapter focused in the microanalysis of the granular fraction, in this section the distribution of AgNPs in major fractions of the SBR will be considered. It is of capital importance to understand how is the distribution of AgNPs in a broader scenario. Therefore, a new experimental design was adopted to quantify the Ag in the mixed-liquor and effluent fractions recurring to different techniques in an attempt to portray a rough mass balance of the AgNPs-fed reactor.

The physical characteristics of the mixed-liquor and effluent fractions require different approaches, which include different analytical techniques to determine Ag concentration in different media. The concentration of Ag in supernatants and effluents may be considerably low than in biomass fractions. Also, sample preparation requirements are totally different in what concerns homogenization of the materials for representative analysis (see Methods section).

Therefore, the Ag concentration solid fractions obtained either by centrifugation (pellets) and filtration were analysed by PIXE, which is an expedite technique to analyse solid samples, whereas supernatants and effluents were analysed by ICP-MS, which has a higher sensitivity than PIXE and is the gold standard technique for the analysis of liquid samples. The concentration of Ag in the input suspension was also analysed by ICP-MS.

A suspension of 100 mg/L AgNPs was continually used as input in the reactor to grant a final concentration of 10mg/L in the Ag-fed bioreactor in each cycle. A sample of this feed input was collected directly at the end of the feeding tube revealing an Ag concentration of 76 mg/L, which is an

acceptable value given the details in the feeding. From the feeding thank, passing through a peristatic pump in a plastic tube until reaching the bioreactor as a final destination, some losses might be expected.

In Table 2 the results of the total reactor content and total effluent fractions obtained by filtration, consisting of solid and liquid fractions are listed.

Table 2. Ag concentration estimated for both mixed liquor and effluent concerning Ag-fed SBR1 and Ag-free control SBR2. Solid fractions were analysed by PIXE and liquid fractions by ICP-MS. Results are in mg/L. *This fraction was subjected to an additional washing and filtration step.

		Ag concentration (mg/L)	
		SBR1	**SBR2**
Mixed liquor	Solid fraction	$1.76x10^{+2}$*	$1.69x10^{0}$
		$2.89x10^{+2}$	NA
	Liquid fraction	$7.00x10^{-2}$	<MDL
		$8.00x10^{-2}$	<MDL
Effluent	Solid fraction	$2.05x10^{+1}$	<MDL
	Liquid fraction	$8.00x10^{-2}$	NA
		$8.00x10^{-2}$	NA

The solid fractions corresponding to the solid residue mainly composed by biomass that is retained in the filter, were analysed by PIXE. The liquid fractions corresponding to the filtrates were analysed by ICP-MS. In the solid fraction of mixed liquor, the Ag concentration was of 288.55 mg/L. To verify the methodology (filtration) and analytical results for Ag concentrations in the solid fraction of the SBR1 mixed liquor, a pool of samples taken in the same week as those reported above in Table 2 were subjected to different sample preparation methods and analysed by PIXE. The solid fraction was separated by centrifugation (4000 rpm, 10 min), lyophilized and the dry material obtained, pelletized and acid digested as previously described. The results obtained for the Ag concentration in the solid fraction were consistent with the filtered sample. The Ag concentration in the pelletized aliquot of the pool was of 147 mg/L, whereas in the digested aliquot was of 187 mg/L, legitimating the filtration procedure as the obtained concentration values are of the same magnitude. In the mixed liquor liquid fraction (corresponding to the filtrate), Ag concentrations displayed much lower values (0.07 and 0.08 mg/L). This indicates that most Ag is retained in the biomass, and not in suspension or dissolved in the liquid fraction.

Concerning the effluent samples, an Ag concentration 20.49 mg/L was found in the SBR1 effluent solid fraction, representing an 8-fold reduction when compared to the homolog mixed liquor solid fraction. The detected Ag concentration in the effluent liquid fraction was 0.08 mg/L, once again indicating that the majority of AgNPs are associated with the biomass. In this single assay, and considering all the silver quantified in the effluent, meaning the Ag concentration in solid and liquid fractions, the liquid fraction only represented 0.38%.

Moreover, when comparing the liquid fractions obtained from the mixed liquor and from the effluent, the Ag contents found were very similar. This suggests an even distribution of Ag content across both liquid fractions of the operational system (mixed liquor and effluent), which is much lower than the correspondent solid portions. Once again, the fact that Ag concentrations in the liquid fraction of both mixed liquor and effluent are similar can indicate that the majority of Ag in the reactor is associated to the mixed liquor solid content, that is to say biomass.

To explore the mobility of Ag in the solid fraction, replicates of the mixed liquor and effluent filtered samples of the Ag-fed system (SBR1) were additionally washed with 10mL of distilled water by filtration and Ag concentration measured in both solid and liquid fractions obtained. The procedure was run in parallel to the samples reported on Table 2. The results obtained were of the same order of magnitude, i.e., 176 mg/L in the mixed liquor solid fraction and of 0.09 mg/L and 0.01 mg/L for the mixed liquor and effluent liquid fractions respectively. Therefore, the additional washing caused a loss of Ag in the mixed liquor solid fraction retained in the filter. This finding suggests that AgNPs in suspension were retained in the solid fraction during the filtration step or a small fraction of AgNPs may be loosely bound to biomass and can be therefore washed out. The test also showed that Ag concentration changes in the liquid fractions were minimal. In addition, the increase in Ag concentration in the filtrate does not reflect the amount of Ag lost in the solid fraction due to the washing procedure. The quantitative results may be affected by a number of uncertainties in the methodological procedure, which can be related to dry deposit weighting, mass loss during washing, among others.

The differences obtained in Ag concentration between the washed and unwashed biomass samples proved that a fraction of Ag may be trapped in the biomass network but not effectively associated to biomass. In fact, without washing we are concentrating the sample, part of the Ag that is being detected in the biomass should be quantified in the supernatant. Therefore, when using filtration to separate the mixed liquor components, an additional washing step may be appropriate. Nevertheless, the methodology should be thoroughly checked in order to confirm its suitability.

Regarding SBR2, the mixed liquor was also tested to detect a possible presence of Ag in the reactor. In ideal conditions no Ag should be detected, however, a residual value was detected indicating minor contamination 1.7 mg/L in the biomass (solid) fraction. This Ag marginal presence was most likely caused by contamination of laboratory containers used in daily manipulation of the reactors. No Ag could be detected in the SBR2 effluent or in the liquid fraction of mixed liquor (Ag detection limit: 1 µg/L).

Some equipment difficulties compromised the number of performed experiments, reducing the desired statistical strength of this study. Thus, the analyses carried out were only exploratory. Replicates of the tests performed would be useful providing statistical power to the results obtained. Nevertheless, the exploratory analysis helped establishing the adequacy of methods and techniques to quantify Ag in the different fractions. Also, the level of Ag concentrations in both solid and liquid fractions provided strong indications about the capacity of biomass to retain AgNPs in a large scale and of the low solubilization of Ag. Clearly, the results obtained in this study cannot be seen as a mass balance. Still, further efforts are needed to test different sampling methodologies in order to attain a more definitive protocol. The use of other techniques, such as ultracentrifugation can be advantageous to study the soluble AgNPs fraction.

As AgNPs are being fed into the reactor the biomass showed to become Ag enriched. An AgNPs input of 10mg/L is provided for each six-hour cycle and the estimated Ag concentration values for biomass showed values in a superior order of magnitude. The values correspond to a cycle from

operational day number 79, but as biomass content appears to stabilize in the tested reactors, the Ag content should also reach a steady concentration value. Further studies are required to confirm this assumption. Nonetheless the large majority of the detected Ag was undoubtedly associated to the biomass.

Conclusions

Regarding the quantification of PN and PS in EPS extracted from AGS SBRs, the overall profile across the totality of the monitored period showed that the concentration values of PN and PS varied randomly through time and were within a limited range. This suggests that the registered alterations were most likely due to the specific reactor dynamic rather than to the presence or absence of AgNPs. No evident trend was observed in a cycle period concerning PN content, but the results on PS content appeared to reveal an incipient pattern, where the total PS content increased in the anaerobic phase (feast phase) and later decrease with aeration (famine phase). This way, the total PS content production and consumption processes across the SBR cycle appear to be, to some extent, related to the external substrate availability. The starvation induced by an 18-day biomass storage appeared to have accentuated this tendency, evident in the first monitored cycle after the hiatus, showing that the PS fraction was consumed during the storage period. The variations of both PN and PS were identical for SBR1 and SBR2, indicating that the AgNPs presence did not affect the overall EPS profile across a reaction cycle.

The SBR2 granules displayed a decreased concentration gradient of structural elements towards the core of the granule, while micronutrients showed a tendency to be more concentrated at the periphery of the granules. The elemental distributions in SBR1 granules showed a different pattern, which for most of the structural elements is opposite to SBR2. In SBR1 granules exposed to AgNPs, the Ag distribution showed a preferential deposition at the periphery with a sharp decrease to inner regions of the granule.

Nevertheless, the preferential Ag deposition observed at the periphery of the granule sharply decreased towards the core of the granule. Also, Ag was found to be retained in the biomass in large scale, and only a very small fraction of Ag seemed to be solubilized or in suspension in the liquid fraction of the reactor. Altogether, the differences in elemental profiles enabled to differentiate granules exposed to AgNPs and importantly defined a signature for different regions of the granular structures. The elemental profiles and their associations with outer or inner regions of the granule seem to indicate that the external layers of the granule act as a barrier to AgNPs, protecting the microbiological communities of inner regions from potential Ag toxic effects. This is also consistent with the increase of structural elements concentration in inner regions of the SBR1 granules, which may reflect a more active metabolism in these regions. These findings may possibly indicate that the increased cellular activity counteract a loss in the capacity of capturing nutrients from media, required to the sustainability of the microbiological communities, due to presence of AgNPs and their binding to EPS. On the other hand, the presence of AgNPs did not significantly influence EPS profile or PS and PN contents in both Ag-fed and Ag-free bioreactors. However, it should be taken into account that the low granular biomass content in both SBR1 and SBR2 may impede the detection of significant changes in EPS contents that can be linked to the metabolic activity of granular biomass. Other aspect that may support the increased metabolic activity of granular biomass in the presence of AgNPs, is the positive effect that AgNPs, at least in the concentration levels used, had in granulation and therefore in the performance of the AGS system.

Future prospects

Future work should focus aspects that will enable setting parameters to estimate the reactor mass balance and process evaluation. This will consist of regular Ag concentration determination in biomass and liquid fractions through the reactor cycles and Ag concentration in the effluent.

Despite being very laborious, the evolution of AgNPs concentration in the reactors, as well as the total EPS content should be studied simultaneously from the granulation phase to a more stable period, possibly enabling the establishment of a relation between the PN/PS content evolution during the granulation and the AgNPs retained in the system.

References

1. Bilińska, L., Gmurek, M. & Ledakowicz, S. Comparison between industrial and simulated textile wastewater treatment by AOPs – Biodegradability, toxicity and cost assessment. *Chem. Eng. J.* **306,** 550–559 (2016).
2. World Trade Organization. *World trade statistical review*. (2016).
3. Windler, L., Height, M. & Nowack, B. Comparative evaluation of antimicrobials for textile applications. *Environ. Int.* **53,** 62–73 (2013).
4. Som, C., Wick, P., Krug, H. & Nowack, B. Environmental and health effects of nanomaterials in nanotextiles and façade coatings. *Environ. Int.* **37,** 1131–1142 (2011).
5. Mueller, N. C. & Nowack, B. Exposure modelling of engineered nanoparticles in the environment. *Environ. Sci. Technol.* **42,** 44447–53 (2008).
6. Radetić, M. Functionalization of textile materials with silver nanoparticles. *J. Mater. Sci.* **48,** 95–107 (2013).
7. Lourenço, N. D. *et al*. Comparing aerobic granular sludge and flocculent sequencing batch reactor technologies for textile wastewater treatment. *Biochem. Eng. J.* **104,** 57–63 (2015).
8. Lourenço, N. D., Novais, J. M. & Pinheiro, H. M. Effect of some operational parameters on textile dye biodegradation in a sequential batch reactor. *J. Biotechnol.* **89,** 163–174 (2001).
9. Weber, S. D., Ludwig, W., Schleifer, K., Fried, J. & Al, W. E. T. Microbial Composition and Structure of Aerobic Granular Sewage Biofilms. *Appl. Environ. Microbiol.* **73,** 6233–6240 (2007).
10. De Kreuk, M. K., Kishida, N. & Van Loosdrecht, M. C. Aerobic granular sludge - State of the art. *Water Sci. Technol.* **55,** 75–81 (2007).
11. Mcswain, B. S., Irvine, R. L., Hausner, M. & Wilderer, P. a. Composition and Distribution of Extracellular Polymeric Substances in Aerobic Flocs and Granular Sludge. *Appl. Environ. Microbiol.* **71,** 1051–1057 (2005).
12. Geyik, A. G. & Çeçen, F. International Biodeterioration & Biodegradation Variations in extracellular polymeric substances (EPS) during adaptation of activated sludges to new feeding conditions. *Int. Biodeterior. Biodegradation* **105,** 137–145 (2015).
13. Bento, J. B. Interaction of silver nanoparticles with aerobic granular sludge in textile wastewater treatment bioreactors. (IST, 2016).
14. Watt, F. *et al.* Whole cell structural imaging at 20 nanometre resolutions using MeV ions. *Nucl. Inst. Methods Phys. Res.* **306,** 6–11 (2013).
15. Jeynes, C. & Colaux, J. L. Thin film depth profiling by

ion beam analysis. *Analyst* **141,** 5944–5985 (2016).
16. Breese, M. B., Jamieson, D. N. & King, P. J. *Materials analysis using a nuclear microprobe*. (John! Wiley & Sons Ltd, 1996).
17. Nastasi, M., Mayer, J. W. & Wang, Y. *Ion beam analysis: fundamentals and applications*. *CRC Press* (2014).
18. Zhang, P. *et al.* Extracellular protein analysis of activated sludge and their functions in wastewater treatment plant by shotgun proteomics. *Nat. Publ. Gr.* 1–11 (2015).
19. Dubois, M., Gilles, K. A., Hamilton, J. K., Rebers, P. A. & Smith, F. Colorimetric Method for Determination of Sugars and Related Substances. *Anal. Chem.* **28,** 350–356 (1956).
20. Pinheiro, T., Duflou, H. & Maenhaut, W. Applicability of microwave acid digestion to sample preparation of biological materials for analysis by particle-induced X-ray emission (PIXE). *Biol Trace Elem Res* **26–27,** 589–97 (1990).
21. Pinheiro, T. *et al.* Elemental Distribution in the Human Respiratory System and Excretion Organs: Absorption and Accumulation. *X-Ray Spectrom.* **26,** 217–222 (1997).
22. Grime, G. W. & Dawson, M. Recent developments in data acquisition and processing on the Oxford scanning proton microprobe. *Nucl. Instruments Methods Phys. Res. Sect. B Beam Interact. with Mater. Atoms* **104,** 107–113 (1995).
23. Van Espen, P., Janssens, K. & Swenters, I. AXIL X-ray analysis software. *Canberra Packard, Benelux* (1986).
24. Reis, M. A. & Alves, L. C. DATTPIXE, a computer package for TTPIXE data analysis. *Nucl. Instruments Methods Phys. Res. Sect. B Beam Interact. with Mater. Atoms* **68,** 300–304 (1992).
25. Wang, Z., Liu, L., Yao, J. & Cai, W. Effects of extracellular polymeric substances on aerobic granulation in sequencing batch reactors. *Chemosphere* **63,** 1728–1735 (2006).
26. Deng, S., Wang, L. & Su, H. Role and influence of extracellular polymeric substances on the preparation of aerobic granular sludge. *J. Environ. Manage.* **173,** 49–54 (2016).
27. Zhu, L., Dai, X., Yu, Y. W., Qi, H. Y. & Xu, X. Y. Role and significance of extracellular polymeric substances on the property of aerobic granule. *Bioresour. Technol.* **107,** 46–54 (2012).
28. Wang, Z., Liu, Y. & Tay, J. Biodegradability of extracellular polymeric substances produced by aerobic granules. *Appl. Microb. CELL Physiol.* **74,** 462–466 (2007).
29. Ortega, R., Devès, G. & Carmona, A. Bio-metals imaging and speciation in cells using proton and synchrotron radiation X-ray microspectroscopy. *J. R. Soc. Interface* **6 Suppl 5,** S649-58 (2009).
30. Sheng, G., Yu, H. & Li, X. Extracellular polymeric substances (EPS) of microbial aggregates in biological wastewater treatment systems : A review. *Biotechnol. Adv.* **28,** 882–894 (2010).
31. Zhang, L., Feng, X., Zhu, N. & Chen, J. Role of extracellular protein in the formation and stability of aerobic granules. *Enzyme Microb. Technol.* **41,** 551–557 (2007).
32. Frølund, B., Palmagren, R., Keiging, K. & Nielsen, P. H. Extraction of extracellular polymers from activated sludge using a cation exchange resin. *Water Res.* **30,** 1749–1758 (1996).
33. Schmidt, J. E. & Ahring, B. K. Extracellular polymers in granular sludge from different upflow anaerobic sludge blanket (UASB) reactors. *Appl. Microbiol. Biotechnol.* **42,** 457–462 (1994).
34. Batstone, D. J. & Keller, J. Variation of bulk properties of anaerobic granules with wastewater type. *Water Res.* **35,** 1723–1729 (2001).
35. Tay, J., Liu, Q. & Liu, Y. The role of cellular polysaccharides in the formation and stability of aerobic granules. *Lett. Appl. Microbiol.* **33,** 222–226 (2001).
36. Wang, Q., Kang, F., Gao, Y., Mao, X. & Hu, X. Sequestration of nanoparticles by an EPS matrix reduces the particle-specific bactericidal activity. *Sci. Rep.* **6,** 1–10 (2016).
37. Kang, F., Alvarez, P. J. & Zhu, D. Microbial extracellular polymeric substances reduce Ag+ to silver nanoparticles and antagonize bactericidal activity. *Environ. Sci. Technol.* **48,** 316–322 (2013).
38. Mu, H., Zheng, X., Chen, Y., Chen, H. & Liu, K. Response of Anaerobic Granular Sludge to a Shock Load of Zinc Oxide Nanoparticles during Biological Wastewater Treatment. *Environ. Sci. Technol.* 5997–6003 (2012).